Inorg. Chem. **2008**, *47*, 10644−10655

Low-Temperature N−O Bond Cleavage of Nitrogen Monoxide in Heterometallic Carbonyl Complexes. An Experimental and Theoretical Study†

M. Esther García,‡ Sonia Melón,‡ Miguel A. Ruiz,*,‡ Ramón López,§ Tomás Sordo,§ Luciano Marchiò,|| and Antonio Tiripicchio||

Departamento de Química Orgánica e Inorgánica/IUQOEM, Universidad de Oviedo, E-33071 Oviedo, Spain, Departamento de Química Física y Analítica, Universidad de Oviedo, E-33071 Oviedo, Spain, and Dipartimento di Chimica Generale ed Inorganica, Chimica Analitica, Chimica Fisica, Università di Parma, Viale G. P. Usberti 17/A, I-43100 Parma, Italy

Received July 19, 2008

The reaction of $Na[RuCp(CO)_2]$ with $[MnCp'(CO)_2(NO)]BF_4$ gives the corresponding heterometallic derivative $[MnRuCpCp'(\mu\text{-}CO)_2(CO)(NO)]$ ($Cp = \eta^5\text{-}C_5H_5$; $Cp' = \eta^5\text{-}C_5H_4Me$). In contrast, the group 6 metal carbonyl anions $[MCp(CO)_2L]^-$ (M = Mo, W; L = CO, $P(OMe)_3$, PPh_3) react with the Mn and Re complexes $[M'Cp'(CO)_2(NO)]BF_4$ to give the heterometallic derivatives $[MM'CpCp'(\mu\text{-}N)(CO)_3L]$ having a nitride ligand linearly bridging the metal centers (W−N = 1.81(3) Å, N−Re = 1.97(3) Å, W−N−Re = 179(1)°, in $[WReCpCp'(\mu\text{-}N)(CO)_3\{P(OMe)_3\}]$). Density-functional theory calculations on the reactions of $[WCp(CO)_3]^-$ and $[RuCp(CO)_2]^-$ with $[MnCp(CO)_2(NO)]^+$ revealed a comparable qualitative behavior. Thus, two similar and thermodynamically allowed reaction pathways were found in each case, one implying the displacement of CO from the cation and formation of a metal−metal bond, the other implying the cleavage of the N−O bond of the nitrosyl ligand and release of a carbonyl from the anion as CO_2. The second pathway is more exoergonic and is initiated through an orbitally controlled attack of the anion on the N atom of the NO ligand in the cation. In contrast, the first pathway is initiated through a charge-controlled attack of the anion to the C atom of a CO ligand in the cation. The CO_2-elimination pathway requires at the intermediate stages a close approach of the NO and CO ligands, which is more difficult for the Ru compound because of its lower coordination number (compared to W). This effect, when combined with a stronger stabilization of the initial intermediate in the Ru reaction, makes the CO_2-elimination pathway slower in that case.

Introduction

Nitrogen monoxide is a remarkable molecule able to strongly bind to transition metal atoms both in high and low oxidation states, thus giving rise to a wide variety of coordination and organometallic complexes exhibiting a rich chemistry.[1,2] Further interest in this molecule stems from its biological activity, also related in many cases to its ability to bind to metal centers.[1,3] In addition, nitrogen monoxide is of great relevance from an environmental point of view, since this substance is released to some extent in all combustion processes, from both stationary and mobile power sources (vehicle engines, power stations, domestic heating, etc.), as well as in some specialized chemical processes (nitric acid production, nitration plants, etc.), thus

† This paper is dedicated to Prof. E. Carmona on the occasion of his 60th birthday.

* To whom correspondence should be addressed. E-mail: mara@uniovi.es.

‡ Departamento de Química Orgánica e Inorgánica/IUQOEM, Universidad de Oviedo.

§ Departamento de Química Física y Analítica, Universidad de Oviedo.

|| Università di Parma.

(1) Ritcher-Addo, G. B.; Legzdins, P. *Metal Nitrosyls*; Oxford University Press: Oxford, U.K., 1992.

(2) (a) Hayton, T. W.; Legzdins, P.; Sharp, W. B. *Chem. Rev.* **2002**, *102*, 935. (b) Ford, P. C.; Lorkovic, I. M. *Chem. Rev.* **2002**, *102*, 993. (c) Mingos, D. M. P.; Sherman, D. J. *Adv. Inorg. Chem.* **1989**, *34*, 293. (d) Gladfelter, W. L. *Adv. Organomet. Chem.* **1985**, *24*, 41.

(3) (a) Franke, A.; Roncaroli, F.; Rudi, v. E. *Eur. J. Inorg. Chem.* **2007**, 773. (b) Ghosh, A. *Acc. Chem. Res.* **2005**, *38*, 943. (c) Ford, P. C.; Laverman, L.; Lorkovic, I. M. *Adv. Inorg. Chem.* **2003**, *54*, 203. (d) Wang, P. G.; Xian, M.; Tang, X.; Wu, X.; Wen, Z.; Cai, T.; Janczuk, A. J. *Chem. Rev.* **2002**, *102*, 1091. (e) Butler, A. R.; Megson, I. L. *Chem. Rev.* **2002**, *102*, 1155. (f) Williams, R. J. P. *Chem. Soc. Rev.* **1996**, 77. (g) Clarke, M. J.; Gaul, J. B. *Struct. Bonding (Berlin)* **1993**, *81*, 147.

10.1021/ic801356m CCC: $40.75
Published on Web 10/18/2008

Chart 1

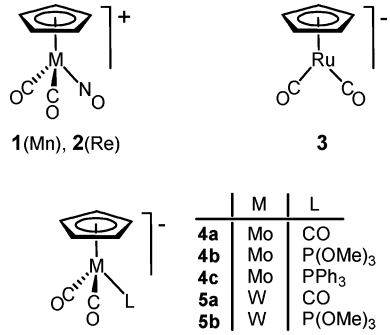

becoming one of the important air pollutants.[1,4,5] In most of these cases, the reduction of NO emissions to desirable levels eventually requires specific final processes for the abatement of this gas, these mainly relying on its selective catalytic reduction (SCR processes), or even decomposition, using diverse heterogeneous catalysts. Yet after the extensive work carried out over the last four decades in search for better, more durable, and less expensive solid catalysts, an intense research on this matter persists at present, on both the academic and the industrial sides.[6] At the heart of all this work is the understanding and control of the activation and cleavage of the N−O bond of nitrogen monoxide when bound to a metal atom, which then becomes a fundamental reaction to be studied at any level, on either solid materials or molecular substances. In this context we have carried out a prospective study on this fundamental reaction using different binuclear carbonyl complexes as potential activators of the N−O bond of the nitrosyl ligand.

The ability of organometallic clusters to cleave the N−O bond of the nitrosyl ligand is known. Thus it is not unusual that the treatment of carbonyl clusters with several sources of the NO ligand would lead to the corresponding nitride (rather than nitrosyl) derivatives.[2c,d] Intermediate nitrosyl complexes are expected to be involved in these reactions, but the actual transformation of a well-defined nitrosyl complex into the corresponding nitride derivative has been rarely observed (eq 1).[7] A few other reactions involving the cleavage of the N−O bond by metals in well-defined organometallic nitrosyl complexes have been reported, all of these involving electron-deficient centers, either binuclear (eq 2)[8] or mononuclear ones (eq 3).[9] Yet, another reported cleavage process is the abstraction of the oxygen atom of a terminal nitrosyl ligand by a strongly oxophilic complex (eq 4).[10]

$$M_n(NO)(CO)_m \rightarrow M_n(\mu\text{-}N)(CO)_{m-1} + CO_2 \quad (1)$$

$$M(\mu\text{-}NO)M \rightarrow M{\equiv}N{-}M(O) \quad (2)$$

$$M(NO)R \rightarrow M(O)(NR) \quad (3)$$

$$L_nM{-}NO + M'L'_m \rightarrow L_nM{\equiv}N{+}M'(O)L'_m \quad (4)$$

In this paper we report our results on the reactions of the electron-precise nitrosyl cations $[MCp'(CO)_2(NO)]^+$ (BF_4^- salts; M = Mn (**1**), Re (**2**); Cp′ = η^5-C_5H_4Me) with several anionic carbonyl complexes of the group 6 and 8 metals having cyclopentadienyl ligands (**3**−**5**, Chart 1). As will be discussed, these reactions take place readily at low temperatures, and they can lead either to metal−metal bonded complexes or to heterometallic nitride-bridged derivatives, depending on the metals involved. A density-functional theory (DFT) study of the likely pathways involved in these reactions has revealed that the formation of the heterometallic metal−metal bonded products is charge-controlled and is initiated through the nucleophilic attack of the anionic metal center on the carbon atom of a carbonyl ligand in the cationic substrate. In contrast, the N−O bond cleavage process yielding the nitride derivative follows from the orbitally controlled nucleophilic attack of the anion on the nitrogen atom of the nitrosyl ligand in the cation, eventually releasing CO_2 (eq 5). These reaction pathways appear not to have been recognized previously in the chemistry of polynuclear complexes having carbonyl or nitrosyl ligands.

$$[L_nM{-}NO]^+ + [M'(CO)L'_m]^- \rightarrow L_nM{\equiv}N{-}M'L'_m + CO_2 \quad (5)$$

Results and Discussion

Group 7/Group 8 Metal Complexes: Metal−Metal Bond Formation. The reactions of the iron complex $Na[FeCp(CO)_2]$ with either the manganese or rhenium nitrosyl compounds $[MCp'(CO)_2(NO)]BF_4$ (**1**, **2**) led to complex mixtures of products that could not be characterized. In contrast, the ruthenium complex $Na[RuCp(CO)_2]$ (**3**) reacts more selectively with the manganese cation **1** (at ca. 223 K in tetrahydrofuran solution) to give the corresponding heterometallic complex $[MnRuCpCp'(\mu\text{-}CO)_2(CO)(NO)]$ (**6**) in medium yield, along with small amounts of the known homonuclear complexes $[Mn_2Cp'_2(CO)_2(NO)_2]$ and $[Ru_2Cp_2(CO)_4]$.[11,12] The latter are most probably derived from

(4) (a) *Reduction of Nitrogen Oxide Emissions*; Ozkan, U. S.; Agarwal, S. K.; Marcelin, G. , Eds.; American Chemical Society: Washington, DC, 1995. (b) *Environmental Catalysis*; Armor, J. M., Ed.; American Chemical Society: Washington, DC, 1994. (c) *Catalytic Control of Air Pollution*; Silver, R. G.; Sawyer, J. E.; Summers, J. C. , Eds.; American Chemical Society: Washington, DC, 1992. (d) *Energy and the Environment*; Dunderdale, J., Ed.; Royal Society of Chemistry: Cambridge, U.K., 1990. (e) *Pollution: Causes, Effects and Control*; Harrison, R. M. , Ed.; Royal Society of Chemistry: Cambridge, U.K., 1990.

(5) (a) Basu, S. *Chem. Eng. Commun.* **2007**, *194*, 1374. (b) Tayyeb, J. M.; Naseem, I.; Gibbs, B. M. *J. Environ. Manage.* **2007**, *83*, 251. (c) Wallington, T. J.; Kaiser, E. W.; Farrell, J. T. *Chem. Soc. Rev.* **2006**, *35*, 335. (d) McMillan, S. A.; Broadbelt, L. J.; Snurr, R. Q. *Environ. Catal.* **2005**, 287. (e) Curtin, T. *Environ. Catal.* **2005**, 197.

(6) For some recent work on this subject, see: (a) Liu, J.; Zhao, Z.; Xu, C.; Duan, A.; Jiang, G. *J. Phys. Chem. C* **2008**, *112*, 5930. (b) Kondratenko, E. V.; Ovsitser, O. *Angew. Chem., Int. Ed.* **2008**, *47*, 3227. (c) Li, Y.; Cheng, H.; Li, D.; Qin, Y.; Xie, Y.; Wang, S. *Chem. Commun.* **2008**, 1470. (d) Liu, F.; Zhang, C. *Chem. Commun.* **2008**, 2043. (e) Pietrzyk, P.; Gil, B.; Sojka, Z. *Catal. Today* **2007**, *126*, 103.

(7) (a) Fjare, D. E.; Gladfelter, W. L. *J. Am. Chem. Soc.* **1984**, *106*, 4799. (b) Feasey, N. D.; Knox, S. A. R.; Orpen, A. G. *J. Chem. Soc., Chem. Commun.* **1982**, 75.

(8) Legzdins, P.; Young, M. A. *Comments Inorg. Chem.* **1995**, *17*, 239.

(9) (a) Blackmore, I. J.; Jin, X.; Legzdins, P. *Organometallics* **2005**, *24*, 4088. (b) Sharp, W. B.; Daff, P. J.; McNeil, W. S.; Legzdins, P. *J. Am. Chem. Soc.* **2001**, *123*, 6272.

(10) (a) Veige, A. S.; Slaughter, LeG. M.; Lobkovsky, E. B.; Wolczansky, P. T.; Matsunaga, N.; Decker, S. A.; Cundari, T. R. *Inorg. Chem.* **2003**, *42*, 6204. (b) Odom, A. L.; Cummins, C. C.; Protasiewicz, J. D. *J. Am. Chem. Soc.* **1995**, *117*, 6613.

(11) James, T. A.; McCleverty, J. A. *J. Chem. Soc., A* **1970**, 850.

Table 1. Selected IR Data for New Compounds[a]

compound	ν(CO)	ν(MN)[b]
[MnRuCpCp′(μ-CO)$_2$(CO)(NO)] (**6**)[c]	1980 (m), 1817 (w), 1782 (vs), 1720 (m)[d]	
[MoReCpCp′(μ-N)(CO)$_4$] (**7a**)	2011 (m), 1950 (vs), 1937 (m), 1906 (m)	908
[MoReCpCp′(μ-N)(CO)$_3${P(OMe)$_3$}] (**7b**)	1945 (m), 1913 (vs), 1877 (m)	921
[MoReCpCp′(μ-N)(CO)$_3$(PPh$_3$)] (**7c**)	1940 (m), 1909 (vs), 1875 (m)	913
[WMnCpCp′(μ-N)(CO)$_4$] (**8**)	2007 (m), 1951 (vs), 1928 (m), 1915 (m)	931
[WReCpCp′(μ-N)(CO)$_4$] (**9a**)	2003 (m), 1941 (vs), 1925 (m), 1898 (m)	937
[WReCpCp′(μ-N)(CO)$_3${P(OMe)$_3$}] (**9b**)	1937 (m), 1904 (vs), 1870 (m)	950

[a] Recorded in petroleum ether solution, unless otherwise stated; ν in cm^{-1}. [b] Data recorded in KBr discs, M = Mo or W. [c] Data recorded in tetrahydrofuran solution. [d] ν(NO).

Chart 2

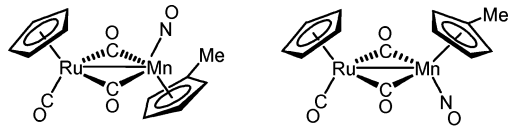

trans-**6** *cis*-**6**

competing electron-transfer side processes, a matter to be addressed later on. The ruthenium complex **3** also reacted with the rhenium cation **2**, but a complicated mixture was obtained and we were not able to isolate or even confirm the presence of the RuRe analogue of complex **6** in these mixtures.

The IR spectrum of complex **6** displays three bands in the C−O stretching region (Table 1). The band at 1980 cm^{-1} denotes the presence of a terminal carbonyl ligand, and those at 1817 (w) and 1782 (vs) cm^{-1} are mainly due to the bridging carbonyls, with their relative intensity being indicative of their almost antiparallel positioning,[13] which is characteristic of flat M$_2$(μ-CO)$_2$ oscillators (Chart 2). Finally, the band at 1720 cm^{-1} can be safely assigned to the N−O stretch of a terminal NO ligand by comparison to that in the dimanganese compound [Mn$_2$Cp′$_2$(CO)$_2$(NO)$_2$] (1711 cm^{-1}).[11]

Even when the ^{1}H NMR spectrum of **6** at room temperature would be consistent with the presence of a single heterometallic species in solution, the ^{13}C NMR spectra denote the presence of dynamic effects, since just a broad carbonyl resonance at 245.8 ppm is observed at 291 K (rather than separated resonances for the bridging and terminal carbonyls). On cooling the solution, this averaged resonance broadens further to disappear at about 248 K, then giving rise at 223 K to separated resonances at 271.7, 198.3, and 197.5 ppm, with relative intensities of about 4:1:1, respectively. At the same time, the cyclopentadienyl resonance broadens, and at 203 K it has split in two resonances of similar intensity. All this is interpreted as the result of the presence in solution of roughly equimolar amounts of two rapidly interconverting and similar isomers, each with two

Chart 3

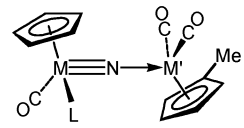

	M	M′	L
7a	Mo	Re	CO
7b	Mo	Re	P(OMe)$_3$
7c	Mo	Re	PPh$_3$
8	W	Mn	CO
9a	W	Re	CO
9b	W	Re	P(OMe)$_3$

bridging and one terminal carbonyl ligand, with accidental (or near) degeneracy in the ^{13}C resonances of the bridging ligands. These can be only the *cis* and *trans* isomers derived from the two possible relative arrangements of the cyclopentadienyl ligands with respect to the M$_2$(μ-CO)$_2$ plane (Chart 2), which is a well-known isomerism in the homonuclear dimers [Mn$_2$Cp′$_2$(CO)$_2$(NO)$_2$] and [Ru$_2$Cp$_2$(CO)$_4$].[14,15] As proposed for these species, it is likely that the *cis*/*trans* interconversion in **6** proceeds via a sequence of bridging to terminal rearrangement of the carbonyl ligands, this being followed by rotation around the intermetallic vector. In this way both *cis*/*trans* isomerization and full scrambling of the carbonyl ligands are achieved, in agreement with the NMR data. Although we have not obtained enough data to accurately calculate the corresponding overall activation barrier, a value of about 40 kJ/mol can be estimated by taking 248 K as the coalescence temperature of the carbonyl resonances.[16] In agreement with this, we have computed that half of this value (4.2 kcal/mol or 18 kJ/mol) corresponds to the Gibbs energy of the barrier converting ***trans*-6** into the corresponding isomer having terminal carbonyls but still transoid arrangement of the Cp ligands (DFT calculations to be discussed later on).

Group 7/Group 6 Metal Complexes: N−O Bond Cleavage. In contrast to the reactions discussed above, those of the nitrosyl complexes **1** and **2** with the molybdenum and tungsten carbonyl anions of type [MCp(CO)$_2$L]$^-$ (**4**,**5**) (Na$^+$ or K$^+$ salts, L = CO, P(OMe)$_3$, PPh$_3$) give as major products the corresponding nitride-bridged derivatives [MM′CpCp′(μ-N)(CO)$_3$L}] (**7**−**9**) (Chart 3), when carried out in tetrahydrofuran or dichloromethane solutions at about 223 K. These products were isolated as pure solids in about 60% (Mn) and 75−80% (Re) yields. We also identified in the corresponding reaction mixtures the presence of small amounts of the respective homonuclear dimers [Mn$_2$Cp′$_2$(CO)$_2$(NO)$_2$][11] and [M$_2$Cp$_2$(CO)$_4$L$_2$] (M = Mo, W),[17] as well as the hydride complexes [MCpH(CO)$_2$L],[18] and other unidentified species. The hydride complexes obviously arise from unwanted hydrolysis of the anions used, while the dimers are most probably derived from competing electron-transfer side

(12) Humphries, A. P.; Knox, S. A. R. *J. Chem. Soc., Dalton Trans.* **1975**, 1710.
(13) Braterman, P. S. *Metal Carbonyl Spectra*; Academic Press: London, U.K., 1975.
(14) Kirchner, R. M.; Marks, T. J.; Kristoff, J. S.; Ibers, J. A. *J. Am. Chem. Soc.* **1973**, *95*, 6602.
(15) Gansow, O. A.; Burke, A. R.; Vernon, W. D. *J. Am. Chem. Soc.* **1976**, *98*, 5817.
(16) Calculated using the modified Eyring equation $\Delta G^{\#} = 19.14T_c[9.97 + \log(T_c/\Delta\nu)]$ (in J/mol). See Günther, H. *NMR Spectroscopy*; John Wiley: Chichester, U.K., 1980, p 243.
(17) (a) Bruce, M. I.; Goodall, B. L.; Sharrocks, D. N.; Stone, F. G. A. *J. Organomet. Chem.* **1972**, *39*, 139. (b) Birdwhistell, R.; Hackett, P.; Manning, A. R. *J. Organomet. Chem.* **1978**, *157*, 239.
(18) (a) Mays, M. J.; Pearson, S. M. *J. Chem. Soc (A)* **1968**, 2291. (b) Manning, A. R. *J. Chem. Soc (A)* **1968**, 651. (c) King, R. B. *Organometallic Synthesis, Vol 1*; Academic Press: London,U. K., p 156.

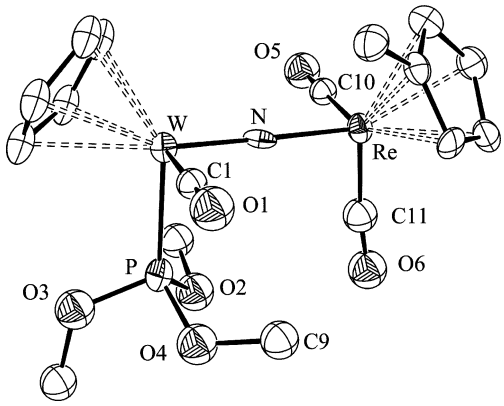

Figure 1. ORTEP drawing (30% probability) of the molecular structure of compound **9b**, with H atoms omitted for clarity.

Table 2. Selected Bond Lengths (Å) and Angles (deg) for Compound **9b**

W−N	1.81(3)	Re−N	1.97(3)
W−C(1)	1.96(3)	Re−C(10)	1.85(3)
W−P	2.36(1)	Re−C(11)	1.83(4)
C(1)−W-P	92(1)	C(10)−Re−C(11)	86(1)
C(1)−W-N	97(1)	C(10)−Re−N	95(1)
P−W−N	90(1)	C(11)−Re−N	98(1)
W−N−Re	179(1)		

processes (see below). The formation of the nitride complexes **7**−**9** is fast at low temperatures and requires the elimination of a carbonyl ligand, presumably as CO_2. In agreement with this, the IR monitoring of the corresponding reaction mixtures revealed the formation of CO_2, identified through its characteristic asymmetric C−O stretching band at 2338 cm^{-1} in CH_2Cl_2 solution (identical to the band exhibited by a CO_2-saturated dichloromethane solution prepared independently). Although several intermediate species might be involved in the formation of the nitride complexes (see DFT calculations to be discussed later on), none of these could be detected through the IR monitoring of these mixtures.

X-ray Structure of Compound 9b. Even if only crystals of poor quality could be grown for one of the nitride-bridged complexes, the MoRe derivative having a $P(OMe)_3$ ligand (**9b**), its molecular structure could be determined by X-ray diffraction. This is shown in the Figure 1, while the most significant bond distances and angles are collected in the Table 2. The molecule is made up of two fragments of type $MCpL_2$ asymmetrically bridged by a nitride ligand in an essentially linear fashion, thus yielding a pseudo-octahedral environment around each metal atom, if assuming the Cp ligands as occupying three facial positions. The W−N length is quite short, 1.81(3) Å, consistent with the triple W≡N bond that could be formulated to achieve an 18-electron count at the tungsten atom. This length is only slightly longer than those measured in related terminal imido complexes such as [WLCl(NR)(CO)] (L = tris(pyrazolyl)borate ligand) (1.78(1) Å),[19a] and [WCp(O)(NR)R] (1.764(5) Å).[19b] Previously characterized complexes having asymmetric and linear nitride bridges usually have metal centers in high oxidation states, and then display even shorter W≡N lengths, for example about 1.68 Å in $[Mo(N)Me_2(O^tBu)(NC_5H_4{}^tBu)]_4$.[20] In contrast, those complexes having symmetrical and linear nitride bridges display longer separations, formally corresponding to M=N double bonds, for instance 1.848(1) Å in $[W_2Cp^*{}_2Me_6(\mu\text{-}N)]$.[21]

Chart 4

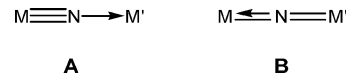

The Re−N length in **9b**, 1.97(3) Å, is considerably shorter than those measured for the N→Re bonds in the rhenium nitride oligomers $[ReNCl_3(POCl_3)]_4$ (2.17 Å) and $[ReNCl_4]$ (2.34 Å)[22] and is also shorter than those for the N→Re bonds in the few complexes of the type $[ReCp(CO)_2L]$ (L = pyridine- or amine-type *N*-donor) characterized so far (2.12−2.23 Å).[23] Moreover, this Re−N length is still about 0.1 Å shorter than that in the acetonitrile complex $[Re_2Cp^*{}_2(\mu\text{-}CO)(CO)_3(NCMe)]$ (2.09(1) Å),[24] a more comparable figure since it involves also an sp-hybridized N atom. On the other hand, the Re−N length in **9b** is yet somewhat longer than those measured for the diazenido complexes $[ReCp\{N_2(C_6H_4OMe)\}(CO)(PMe_3)]$ (1.816(6) Å) and $[ReCl_2(N_2Ph)(PMe_2Ph)_3]$ (1.80 Å),[25] these being taken here as a reference for Re=N double bonds.

On the basis of the above structural features, we trust that there is some π-interaction in the Re−N bond, which of course is detrimental to the N−W π-interaction, so that the binding in the linear core of this complex is surely best represented by a combination of the canonical forms **A** and **B** in Chart 4, yielding bond orders somewhat higher than one (N−Re) and lower than three (N−W), respectively. As it will be discussed below, the DFT-derived molecular orbital (MO) analysis of **9b** is in agreement with this interpretation based on the structural parameters. Finally, we note that the conformation of the molecule is almost an eclipsed one in which each of the bulkier Cp, Cp′, and $P(OMe)_3$ ligands face a carbonyl ligand on the other metal center (**A** in Chart 5).

Structure of the Heterometallic Nitride-Bridged Complexes 7−9. The IR spectra of all complexes **7**−**9**, when recorded in KBr disks, exhibit a broad band in the range 908−950 cm^{-1} which we assign to the M≡N stretch (M = Mo, W) of the nitride ligand. These frequencies are somewhat lower than the values previously reported for coordination compounds having asymmetric nitride bridges, the

(19) (a) Powell, K. R.; Pérez, P. J.; Luan, L.; Feng, S. G.; White, P. S.; Brookhart, M.; Templeton, J. L. *Organometallics* **1994**, *13*, 1851. (b) Legzdins, P.; Rettig, S. J.; Ross, K. J.; Veltheer, J. E. *J. Am. Chem. Soc.* **1991**, *113*, 4361.

(20) Herrmann, W. A.; Bogdanovic, S.; Behm, J.; Denk, M. *J. Organomet. Chem.* **1992**, *430*, C33.

(21) Glassman, T. E.; Liu, A. H.; Schrock, R. R. *Inorg. Chem.* **1991**, *30*, 4723.

(22) Dehnicke, K.; Strähle, J. *Angew. Chem., Int. Ed. Engl.* **1981**, *20*, 413.

(23) (a) Pyshnograeva, N. I.; Setkina, V. N.; Andrianov, V. G.; Struchkov, Y. T.; Kursanov, D. N. *J. Organomet. Chem.* **1978**, *157*, 431. (b) Enders, M.; Kohl, G.; Pritzkow, H. *J. Organomet. Chem.* **2001**, *622*, 66. (c) Wang, T. F.; Hwu, C.; Wen, Y. *J. Organomet. Chem.* **2004**, *689*, 411.

(24) Casey, C. P.; Carino, R. S.; Sakaba, H.; Hayashi, R. K. *Organometallics* **1996**, *15*, 2640.

(25) (a) Cusanelli, A.; Batchelor, R. J.; Einstein, F. W. B.; Sutton, D. *Organometallics* **1994**, *13*, 5096. (b) Duckworth, V. F.; Douglas, P. G.; Mason, R.; Shaw, B. L. *J. Chem. Soc., Chem. Commun.* **1970**, 1083.

Chart 5

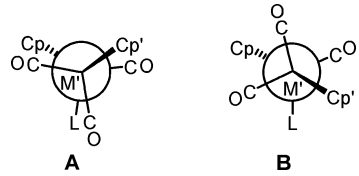

difference being explained by taking into account the lower oxidation state of the metal atoms in our complexes and perhaps also the significant delocalization of the π-bonding interaction along the M−N−M′ axis, already mentioned.

In solution, the IR and NMR data for compounds **7**−**9** (Table 1 and Experimental Section) suggest that they have structures essentially consistent with the one determined for **9b** in the crystal, except for some fine details. As expected, the tetracarbonyl complexes **7a**, **8**, and **9a** give rise to four C−O stretching bands in the corresponding IR spectra, but their relative intensities (m, vs, m, and m, in order of decreasing frequencies) are not those expected from independent *cis*-$M(CO)_2$ oscillators,[13] since that would yield four bands of comparable intensities in each case. This suggests a strong vibrational coupling between both metal fragments in each case, which is consistent with their connection through a strongly bound nitride ligand. However, the NMR data for the tetracarbonyl compounds are indicative of a symmetry in solution somewhat higher than that corresponding to the eclipsed structure found for the tricarbonyl **9b** in the crystal (**A** in Chart 5). Indeed, such a structure would imply the chemical inequivalence within the pairs of carbonyls on each metal center as well as the inequivalence of all CH sites of the methylcyclopentadienyl ring. In contrast to these predictions, the ^{1}H NMR spectra of all our tetracarbonyl compounds display only two distinct CH(Cp′) resonances in each case, and the ^{13}C NMR spectrum of the WRe complex **9a** reveals the presence of pairs of equivalent carbonyl ligands on both the W (δ 226.1 ppm) and Re (δ 203.4 ppm) atoms, as well as pairs of equivalent CH(Cp′) carbon atoms (δ 91.7 and 89.5 ppm). All the above data suggest that, in solution, the tetracarbonyl complexes **7a**, **8**, and **9a** either adopt a staggered conformation (**B** in Chart 5), more symmetrical than the eclipsed one found in the crystal for **9b**, or that the eclipsed conformation **A** allows for the fast rotation of the M′Cp′$(CO)_2$ fragment around the almost single N−M′ bond (this effectively generates an apparent plane of symmetry). To distinguish between these two possibilities we recorded different ^{13}C NMR spectra of **9a** in the range 298−173 K. Unfortunately no significant changes were detected within that range, so we cannot exclude either option. The fact that no more than four (for tetracarbonyl complexes) or three (for tricarbonyl complexes) C−O stretching bands are observed for these compounds even when recording the IR spectra in petroleum ether (this yielding very sharp bands) points to the absence of significant amounts of other rotamers in solution. This would suggest that the staggered conformation **B** might be dominant in solution. Against this, the DFT optimized structure of the WRe tetracarbonyl complex **9a** corresponds to the eclipsed conformation of type **A**, as it will be discussed next.

The presence of a phosphorus-donor ligand in the tricarbonyl complexes **7b,c** and **9b** removes any symmetry element irrespective of whether fast rotation around the N−M′ axis is taking place or not. Indeed, the ^{1}H NMR spectra of all these complexes display more than two CH(Cp′) resonances, and the ^{13}C NMR spectrum of the triphenylphosphine complex **7c** displays three distinct carbonyl resonances and four distinct CH(Cp′) resonances, as expected.

DFT Study on the Reaction Pathways: The WMn System. With the aim of determining the mechanisms operating in those reactions of the cations **1**,**2** with the anions **3**−**5**, and to identify the factors promoting the formation of metal−metal bonds (Mn/Ru system) or the cleavage of the N−O bond of the nitrosyl ligand (Mn,Re/Mo,W systems), we undertook a theoretical investigation of the reactions in tetrahydrofuran solution of the anions $[WCp(CO)_3]^-$ and $[RuCp(CO)_2]^-$ with the cation $[MnCp(CO)_2(NO)]^+$, the latter being taken here as a simplified model of the methylcyclopentadienyl complex **1** actually used in our reactions. The Figures 2 to 5 give the corresponding Gibbs energy profiles in solution, with values given with respect to the separate reactants (see Experimental Section for computational details). The structures of all intermediates and transition states located are also shown in these figures, along with some relevant interatomic distances.

We have found two reactive channels for the approach of $[WCp(CO)_3]^-$ to $[MnCp(CO)_2(NO)]^+$ (Figures 2 and 3). The first channel implies the N−O bond cleavage and eventual release of CO_2 and is initiated by the attack of the W atom of the anion on the N atom of the nitrosyl ligand in the cation, to initially yield the intermediate **I1-co2-w** (−5.3 kcal/mol) having an asymmetric nitrosyl bridge (N−Mn = 1.903 Å, N−W = 2.365 Å) but no metal−metal interaction (Mn−W = 3.875 Å). According to a configuration analysis with the ANACAL program (see Experimental Section for details) the electronic structure of **I1-co2-w** is mainly determined by important ditransferred and monotransferred configurations from the highest occupied molecular orbital (HOMO) of $[WCp(CO)_3]^-$, which presents an important contribution from the d_{xy} orbital of W, to the lowest unoccupied molecular orbital (LUMO) of $[MnCp(CO)_2(NO)]^+$, which exhibits an appreciable contribution from the antibonding π^* orbital of the NO ligand (see Figure 6). As a result, the formation of this intermediate implies an important charge transfer of about 1.3 e from the anionic reactant. It is interesting to note that we have also located a critical structure corresponding to a complex between $[WCp(CO)_3]^-$ and $[MnCp(CO)_2(NO)]^+$ in which the two metal atoms interact with each other at a distance of 3.377 Å. Although this complex has an electronic energy 69.8 kcal/mol below that of the separate reactants, it becomes a transient structure in solution, with a Gibbs energy 16.9 kcal/mol above that of the reactants. Moreover, intrinsic reaction coordinate (IRC) calculations clearly indicate that this complex structure does not belong to the reaction coordinate for the process being investigated by us. No

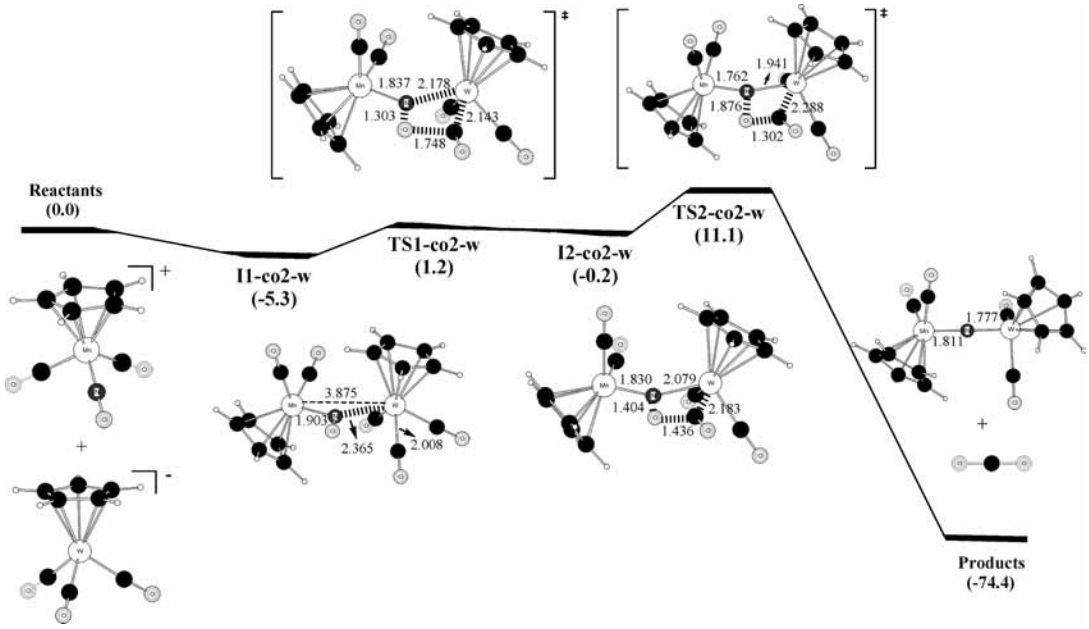

Figure 2. Gibbs energy profile (kcal/mol) in tetrahydrofuran solution, at 253.15 K and 1 atm, for the reaction between $[MnCp(CO)_2(NO)]^+$ and $[WCp(CO)_3]^-$ to give $[MnWCp_2(\mu\text{-}N)(CO)_4]$ and CO_2. Only the most relevant distances (Å) shown.

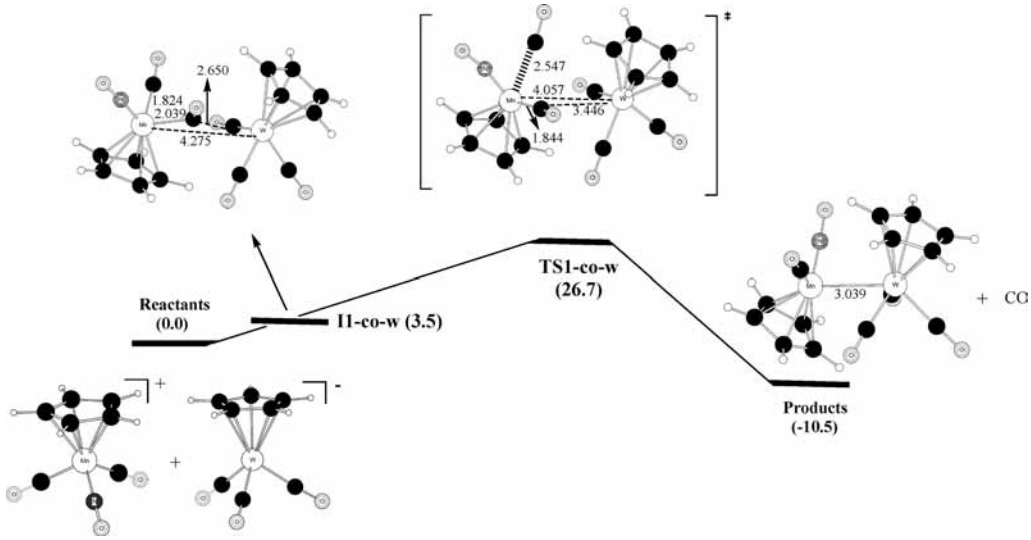

Figure 3. Gibbs energy profile (kcal/mol) in tetrahydrofuran solution, at 253.15 K and 1 atm, for the reaction between $[MnCp(CO)_2(NO)]^+$ and $[WCp(CO)_3]^-$ to give $[MnWCp_2(NO)(CO)_4]$ and CO. Only the most relevant distances (Å) shown.

minimum-energy structures were located having two ligands (CO or NO) bridging the metal atoms.

The intermediate **I1-co2-w** proceeds through the transition state (TS) **TS1-co2-w** (1.2 kcal/mol) for the closer approach of W to the N atom (N−W = 2.178 Å), this also implying an incipient interaction between the O atom of the nitrosyl bridge and the C atom of one of the carbonyls at the tungsten center (O···C = 1.748 Å). This leads to the intermediate **I2-co2-w** (−0.2 kcal/mol) now having a NOCW metallacycle ring with similar O−N (1.404 Å) and O−C (1.436 Å) separations that can be classified as single-bond lengths. Finally, **I2-co2-w** evolves through the TS**TS2-co2-w** with an energy barrier of 16.4 kcal/mol for CO_2 elimination and formation of $[MnWCp_2(\mu\text{-}N)(CO)_4]$. This is the step at which the N−O bond of the nitrosyl ligand (progressively stretched to the point of a single bond at the intermediate **I2-co2-w**) is definitively cleaved, and it is also the rate-determining step. The overall process is quite exoergonic (by 74.4 kcal/mol), thanks mainly to the formation of the very stable CO_2molecule.

In the final MnW complex, the conformation is an eclipsed one similar to that found experimentally for the tricarbonyl ReW compound **9b**. The N−W length (1.777 Å) is only slightly shorter than the corresponding distance measured in **9b** (1.81(3) Å), so it is the N−Mn length (1.811 Å, to be compared to N−Re = 1.97(3) Å in **9b**), if we allow for the about 0.12 Å difference in the covalent radii of Mn and Re.[26] As stated above, we have interpreted the experimental N−M lengths in **9b** as indicative of bond orders somewhat lower than three (N−W) and higher than one (N−Re) respectively, possibly because of some delocalization of the π-bonding interaction along the M−N−M′ axis. In agreement with this,

(26) Cordero, B.; Gómez, V.; Platero-Prats, A. E.; Revés, M.; Echeverría, J.; Cremades, E.; Barragán, F.; Alvarez, S. *Dalton Trans.* **2008**, 2832.

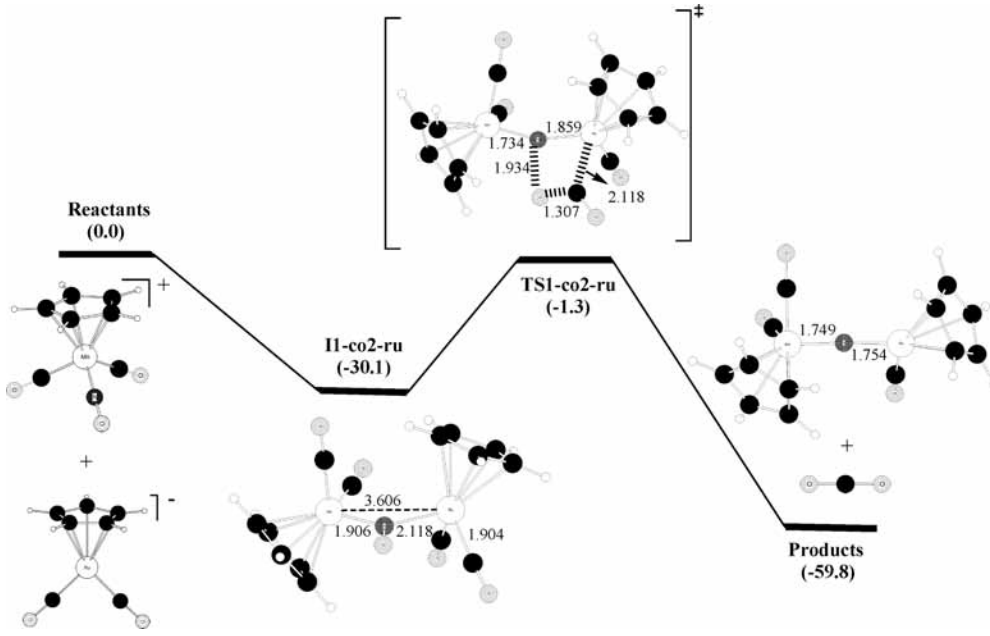

Figure 4. Gibbs energy profile (kcal/mol) in tetrahydrofuran solution, at 253.15 K and 1 atm, for the reaction between $[MnCp(CO)_2(NO)]^+$ and $[RuCp(CO)_2]^-$ to give $[MnRuCp_2(\mu\text{-}N)(CO)_3]$ and CO_2. Only the most relevant distances (Å) shown.

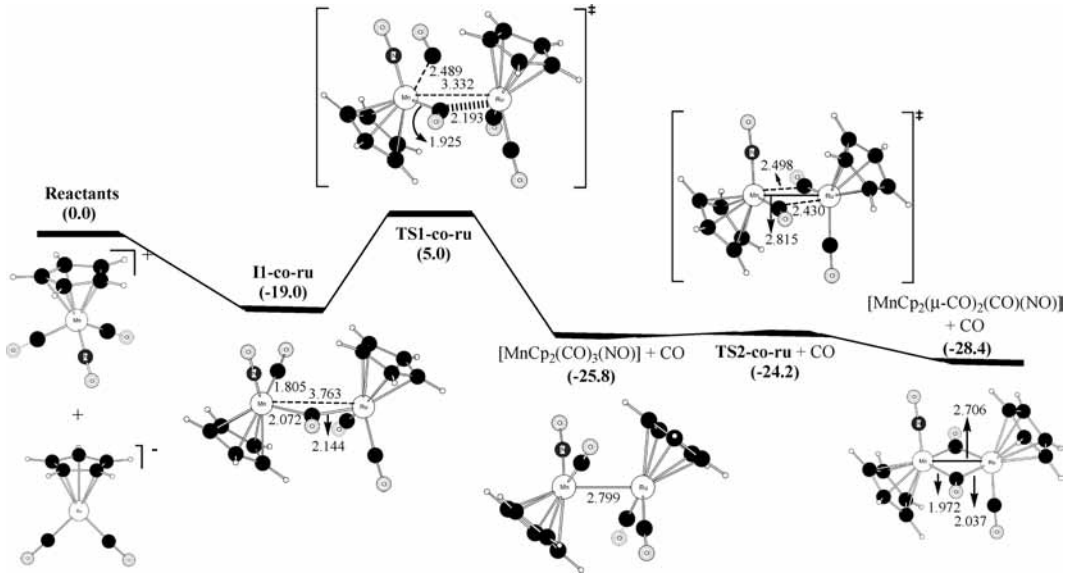

Figure 5. Gibbs energy profile (kcal/mol) in tetrahydrofuran solution, at 253.15 K and 1 atm, for the reaction between $[MnCp(CO)_2(NO)]^+$ and $[RuCp(CO)_2]^-$ to give $[MnRuCp_2(\mu\text{-}CO)_2(CO)(NO)]$ and CO. Only the most relevant distances (Å) shown.

an inspection of the frontier MOs for the computed MnW complex reveals that one of the orbitals describing the π-interaction of the nitride ligand with the metal centers (HOMO−4) is partially delocalized over the Mn−N−W skeleton (Figure 7). We must note here that a similar conclusion was reached on the basis of the experimental data and DFT calculations on the cation $[Mo_2Cp_2(\mu\text{-}P)(CO)_2(\eta^6\text{-}HR^*)]^+$, ($R^* = 2,4,6\text{-}C_6H_2{}^tBu_3$),[27] which displays a phosphide ligand linearly bridging 15-electron and 17-electron Mo fragments and is isoelectronic to the nitride complexes **7**−**9**. Besides, this partial delocalization of the π-interaction of the nitride ligand is perhaps also responsible for the eclipsed conformation computed for the MnW complex (and experimentally observed for **9b**), since it can be guessed that such a delocalization would be greatly removed by the relative rotation of the $MCpL_2$ fragments by about 60°, as required to reach a staggered conformation starting from the eclipsed one (Chart 5).

The second reactive channel in the reaction of $[WCp(CO)_3]^-$ with $[MnCp(CO)_2(NO)]^+$ corresponds to the attack of the W atom of the anion on the C atom of a carbonyl ligand in the cation (Figure 3). According to a configuration analysis, the start of this channel corresponds to the interaction of the HOMO of $[WCp(CO)_3]^-$ with the LUMO+6 of $[MnCp(CO)_2(NO)]^+$, which presents an important contribution from the attacked C−O π^* antibonding orbital (Figure 6). This LUMO+6 preferentially stabilizes owing to the polarization induced by the approach of the anion, thus

(27) Amor, I.; García-Vivó, D.; García, M. E.; Ruiz, M. A.; Sáez, D.; Hamidov, H.; Jeffery, J. C. *Organometallics* **2007**, *26*, 466.

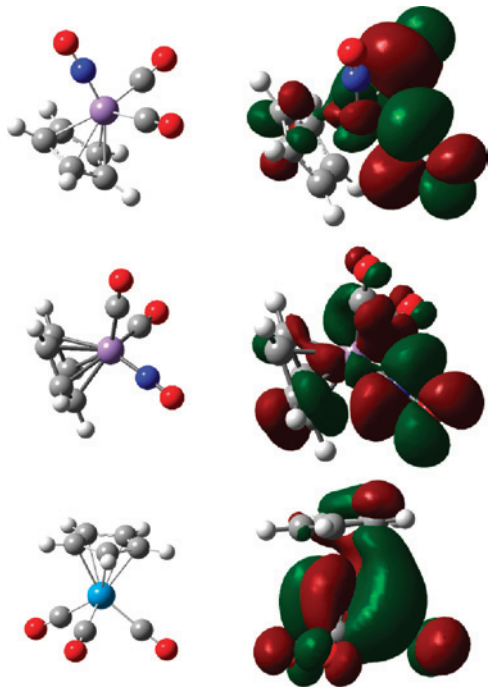

Figure 6. From top to bottom: LUMO+6 and LUMO of the cation $[MnCp(CO)_2(NO)]^+$, and the HOMO in the anion $[WCp(CO)_3]^-$, with the molecular perspective used in each case shown on the left.

Table 3. Atomic Charges (NBO/Mulliken) Calculated for the Complexes $[MnCp(CO)_2(NO)]^+$, $[WCp(CO)_3]^-$, and $[RuCp(CO)_2]^-$

	Mn	W	Ru
M	−0.31/−0.01	−0.15/−0.07	−0.32/−0.37
C(O)	0.66/0.34	0.44/0.18	0.51/0.22
O(C)	−0.35/−0.17	−0.56/−0.40	−0.58/−0.38
N(O)	0.40/0.21		
O(N)	−0.06/−0.09		

becoming the LUMO in the distorted $[MnCp(CO)_2(NO)]^+$ fragment. In the same line, we note that the positive charge of the C(carbonyl) atoms in the cation is higher than the positive charge of the N atom of the nitrosyl ligand in the same molecule, so we can conclude that the approach of the W atom to the C(carbonyl) atom is favored (over the approach to the N atom) on electrostatic grounds (Table 3). This interaction gives rise to an intermediate **I1-co-w** in electronic energy, which becomes a transient species (3.5 kcal/mol) when taking into account solvent effects. At this intermediate the distance between W and the incipiently attacked C(CO) atom is 2.650 Å, and the Mn−W distance is 4.275 Å, too long to be considered yet as bonding, while the charge transfer from the anion is computed to be 0.77 e. The system then evolves by further approach of the W atom to the Mn center and the simultaneous and progressive displacement of a carbonyl ligand out of the coordination sphere of the cation. The corresponding transition state **TS1-co-w** is placed 26.7 kcal/mol above the reactants and defines the overall kinetic barrier, then evolving to the final products. These are now the metal−metal bonded complex $[MnWCp_2(NO)(CO)_4]$ (Mn−W = 3.039 Å) and CO, and the overall process is exoergonic, but only by 10.5 kcal/mol.

Thus, according to the above results both routes (the one leading to the metal−metal bonded product with elimination

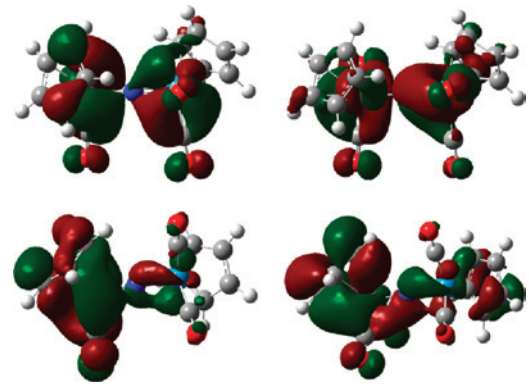

Figure 7. HOMO (upper left), HOMO−1 (upper right), HOMO−3 (lower left), and HOMO−4 (lower right) of the complex $[MnWCp_2(\mu\text{-}N)(CO)_4]$. The W atom is placed on the right in all the views.

of CO, and the one involving the cleavage of the NO ligand and elimination of CO_2) are thermodynamically viable for the reaction between $[WCp(CO)_3]^-$ and $[MnCp(CO)_2(NO)]^+$, although the route involving the elimination of CO_2 is much more exoergonic (by ca. 65 kcal/mol). However, the fact that this reaction gives $[MnWCp_2(\mu\text{-}N)(CO)_4]$ as the only product essentially has a kinetic origin, since the CO_2-elimination channel exhibits a Gibbs energy barrier 10.3 kcal/mol lower than the CO-elimination channel, thus explaining why no metal−metal bonded products (other than small amounts of homonuclear complexes) have been detected in the reactions of the group 6 metal anions **4** and **5** with the group 7 metal cations **1** and **2**.

DFT Study on the RuMn System. For the reaction between $[RuCp(CO)_2]^-$ and $[MnCp(CO)_2(NO)]^+$ we also found two channels analogous to those described above for the MnW system. However, it is interesting to remark that the corresponding Gibbs energy profiles in solution involve species with lower energy than before.

The CO_2-elimination channel (Figure 4) is initiated by the attack of the Ru atom of the anion on the N atom of the nitrosyl ligand in the cation, to give a very stable nitrosyl-bridged intermediate **I1-co2-ru** (−30.1 kcal/mol) in which the N−Ru (2.118 Å) and Mn−Ru (3.606 Å) lengths are clearly shorter than those found in the MnW system, although the intermetallic separation is yet too long to be considered as bonding. As before (**I1-co2-w**) the main fragment configurations describing **I1-co2-ru** are the HOMO($[RuCp(CO)_2]^-$)−LUMO($[MnCp(CO)_2(NO)]^+$) ditransferred and monotransferred configurations, which determine a charge transfer of 1.32 e from the anion. The intermediate **I1-co2-ru** then transforms analogously into $[MnRuCp_2(\mu\text{-}N)(CO)_3]$ through a TS having a NOCRu metallacycle (**TS1-co2-ru**), thus completing the N−O bond cleavage of the original nitrosyl ligand with concomitant ejection of CO_2. The energy barrier for this N−O bond cleavage step (28.8 kcal/mol) accounts for the overall kinetic barrier and is considerably higher than the analogous overall barrier computed for the MnW system (16.4 kcal/mol). Finally, as found for the mentioned system, the overall reaction giving the nitride-bridged complex is quite exoergonic (59.8 kcal/mol). Yet, we must recall that this product has not been detected in the reactions of the anion **3** with the cation **1**.

The CO-elimination channel is again initiated by the nucleophilic attack of the Ru atom of the anion on one of the C(CO) atoms in the cation. A quite stable (−19.0 kcal/mol) carbonyl-bridged intermediate **I1-co-ru** initially forms, in which the Ru−C(CO) distance is 2.144 Å, while the Mn−Ru distance is still nonbonding (3.763 Å), and the charge transfer from the anion amounts to 1.02 e. Again **I1-co-ru** can be described in terms of ditransferred and monotransferred HOMO($[RuCp(CO)_2]^-$)−LUMO($[MnCp(CO)_2(NO)]^+$)configurations where the LUMO of the distorted $[MnCp(CO)_2(NO)]^+$ fragment correlates with the LUMO+6 in the isolated reactant (Figure 6). In the same line, since the positive charge of the C(carbonyl) atoms in the cation is higher than that of the N atom we conclude that the approach of the Ru atom to the C atom is favored on electrostatic grounds, an effect enhanced by the higher negative charge at the Ru center (when compared to W, see Table 3). The intermediate **I1-co-ru** then evolves analogously through the TS **TS1-co-ru** for CO elimination with a Gibbs energy barrier of 24.0 kcal/mol to yield $[MnRuCp_2(NO)(CO)_3]$, placed 25.8 kcal/mol below the reactants. In agreement with our experimental observations, we found that $[MnRuCp_2(NO)(CO)_3]$, a metal−metal bonded structure (Mn−Ru = 2.799 Å) having terminal NO and CO ligands, is not the most stable form, and indeed evolves almost without kinetic barrier (1.6 kcal/mol) through the TS **TS2-co-ru** to finally give the more stable isomer $[MnRuCp_2(\mu\text{-}CO)_2(NO)(CO)]$, this having two bridging carbonyl ligands and a transoid arrangement of the Cp ligands, in agreement with the structural data already discussed for compound **6**. The small barriers connecting the bridgded and unbridged forms of this product are in full agreement with the fluxional behavior displayed by compound **6** in solution, as discussed above. Finally, we note that the reaction leading to $[MnRuCp_2(\mu\text{-}CO)_2(NO)(CO)]$ is exoergonic by 28.4 kcal/mol.

Thus, our theoretical results predict that in the reaction of $[RuCp(CO)_2]^-$ with $[MnCp(CO)_2(NO)]^+$ in tetrahydrofuran solutions both reaction channels are thermodynamically viable. The CO_2-elimination channel involving the N−O bond cleavage of the nitrosyl ligand is more exoergonic (−59.8 vs −28.4 kcal/mol) but it is kinetically less favored, with a Gibbs energy barrier in solution 4.8 kcal/mol higher than that of the CO-elimination channel and involving the formation of the Ru−Mn bond. This is in agreement with the fact that the reaction of the anion **3** with **1** gives only the metal−metal bonded complex **6**, with no detectable amounts of the hypothetical nitride-bridged product emerging from the CO_2-elimination pathway. Since the initial attack of the Ru anion on either the nitrosyl or the carbonyl ligands of the Mn cation has no kinetic barriers, then the relative proportion of the two pathways would be initially determined by statistics, that is, about 67% for the attack to CO and 33% for the attack to NO. This is in good agreement with the experimental yield of 52% for **6** (after crystallization). However, compound **I1-co2-ru** might also be viewed as a reaction product, since the barrier of 29 kcal/mol ensures that it cannot evolve via CO_2 elimination. We cannot offer a fully satisfactory explanation to its absence in the reaction mixture, perhaps derived from a high air-sensitivity that would induce its decomposition during the reaction or upon manipulation of the reaction mixture.

Overall View of the Reaction Pathways Leading to the Heterometallic Complexes 6−9: Concluding Remarks. The displacement of CO in a neutral or cationic carbonyl complex through its reaction with a metal carbonyl anion (sometimes called "redox-condensation") is a widely used synthetic procedure for creating new heteronuclear M−M′ bonds,[28] but the operative mechanisms have been not generally established. Previous studies on these reactions indicate that single[29,30] and even double electron-transfer processes[30] take place between the reacting carbonyl anions and cations, possibly via a carbonyl-bridged intermediate derived from the nucleophilic attack of the anion on a C(carbonyl) atom of the cation. The single electron-transfer processes give rise to neutral radicals then coupling to each other rapidly to give the corresponding metal−metal bonded products, both homonuclear (M−M, M′−M′) and heteronuclear ones (M−M′). Our experimental results indicate that this type of mechanisms are only marginally operative in the reactions of the anions **2**−**5** with the cations **1** and **2** to give the heterometallic compounds **6**−**9**, since only small amounts of the homonuclear products $[Mn_2Cp'_2(CO)_2(NO)_2]$, $[Ru_2Cp_2(CO)_4]$, and $[M_2Cp_2(CO)_4L_2]$ (M = Mo, W) are formed in these reactions. For the single case in which a metal−metal bonded product is formed in our reactions (the MnRu complex **6**), our DFT calculations indeed support the previous hypothesis that the reaction is initiated by the nucleophilic attack of the anion on the C(carbonyl) atom in the cation.[30] However, we find that this intermediate does not evolve through a full electron-transfer to give mononuclear radicals, but just through the progressive labilization of one of the CO ligands at the (former) cationic center as the metal atoms further approach to each other (Figure 5). The same can be said of the reaction pathway leading to the hypothetical formation of the Mn−W bond in the reaction of $[WCp(CO)_3]^-$ with $[MnCp(CO)_2(NO)]^+$ (Figure 3). Thus we must claim that, depending on the reagents used, the "redox condensation" between metal carbonyl anions and cations leading to the formation of heteronuclear M−M′ bonds are likely to be initiated by the nucleophilic attack of the metal atom in the anion on the C atom of a carbonyl ligand in the cation but does not necessarily imply an electron-transfer process, and certainly not in the reactions of the anions **3**−**5** with the nitrosyl cations **1** and **2**.

The formation of a nitride-bridged complex (i.e., the formation of compounds **7**−**9**) by the reaction of a metal carbonyl anion with a cationic nitrosyl complex has no precedent in the literature. As discussed above, this reaction is initiated through an orbitally controlled nucleophilic attack of the metal atom of the anion on the N atom of the nitrosyl

(28) Adams, R. D. In *Comprehensive Organometallic Chemistry II*; Abel, E. W.; Stone, F. G. A.; Wilkinson, G., Eds.; Elsevier: Oxford, U.K., 1995; Vol *10*, Chapter 1.
(29) Lee, K. Y.; Kochi, J. K. *Inorg. Chem.* **1989**, *28*, 567.
(30) (a) Zhen, Y.; Feighery, W. G.; Lai, C. K.; Atwood, J. D. *J. Am. Chem. Soc.* **1989**, *111*, 7832. (b) Zhen, Y.; Atwood, J. D. *J. Am. Chem. Soc.* **1989**, *111*, 1506.

ligand in the cation. Although this elemental step is itself unprecedented, we note that earlier MO calculations on the related cation $[ReCp(NO)(CO)(PPh_3)]^+$ led to the similar conclusion that the hydride attack on this cation to give the formyl derivative $[ReCp(NO)(CHO)(PPh_3)]$ would not occur directly at the C position, but rather at the N atom of the nitrosyl ligand, the main contributor to the LUMO of the Re cation.[31]

When comparing the behavior of the Ru and W anions toward the manganese cation $[MnCp(CO)_2(NO)]^+$ we find a similar qualitative behavior. The quantitative aspects are the ones making the difference and eventually leading to quite different products as a result of the distinct kinetic barriers then generated. Thus, two similar and thermodynamically allowed reaction pathways are found in each case, the CO-elimination channel leading to the metal−metal bonded product, and the CO_2-elimination channel involving the cleavage of the N−O bond. The second channel is in both cases more exoergonic and is initiated through an orbitally controlled interaction between the reagents. In contrast, the first channel is initiated through a charge-controlled interaction leading to a smaller stabilization of the system (by some 10 kcal/mol, in both cases). The main differences between the Ru and W reactions are in part derived from the much stronger interaction of the Ru anion with the Mn cation at either the N or the C positions. Thus, after the attack to the C atom, the RuMn system is more stabilized than the WMn system (−19.0 kcal/mol vs +3.5 kcal/mol, Figures 3 and 5), although this difference has no significant influence on the overall kinetic barriers along this pathway. After the attack on the N atom, the RuMn system is even more stabilized than before (−30.1 kcal/mol vs −5.3 kcal/mol, Figures 2 and 4). This difference, however, when combined with a higher energetic cost to reach the metallacycle intermediate in the RuMn system (**TS1-co2-ru** in Figure 4) yields in this case a high barrier for the CO_2-elimination channel, then rendering the CO-elimination channel faster, thus justifying the formation of compound **6** and the absence of N−O bond cleavage products for the RuMn system. The relative difficulty to reach the metallacycle intermediate for the RuMn system might be just derived from the lower coordination number at Ru (compared to W), this initially placing the bridging nitrosyl and the carbonyl at Ru more separated from each other than are in the W intermediate, then increasing the energetic cost of the approach of the O(N) atom to the C(O) atom. In all, it seems that the success of the group 6 metal anions of the type $[MCp(CO)_2L]^-$ to cleave the N−O bond of the nitrosyl ligand in the group 7 metal cations of type $[M'Cp(CO)_2(NO)]^+$ would be due to the combination of two effects: (a) an initial interaction of medium-strength between the anion and cation and (b) a closer approach of the carbonyl ligands to the bridging nitrosyl in the intermediate initially formed, as a result of the higher coordination number of the group 6 metal atoms. Further work will be needed to prove the generality and use of the above ideas for a better understanding of the ways in which transition-metal complexes can cleave the strong bond of the NO molecule.

(31) Fenske, R. F.; Milletti, M. C. *Organometallics* **1986**, *5*, 1243.

Experimental Section

General Procedures and Starting Materials. All manipulations and reactions were carried out under a nitrogen (99.995%) atmosphere using standard Schlenk techniques. Solvents were purified according to literature procedures and distilled prior to their use.[32] Petroleum ether refers to that fraction distilling in the range 338−343 K. Compounds $[MCp'(CO)_2(NO)]BF_4$ [M = Mn (**1**),[33] Re (**2**)[34]], $Na[RuCp(CO)_2]$ (**3**),[35] $K[MCp(CO)_3]$ [M = Mo (**4a**), W (**5a**)],[36] and $Na[MCp(CO)_2L]$ [L = $P(OMe)_3$; M = Mo (**4b**), W (**5b**).[18b] L = PPh_3; M = Mo (**4c**)],[17a] were prepared as described previously. Chromatographic separations were carried out using jacketed columns cooled by tap water (ca. 285 K). Commercial aluminum oxide (Aldrich, activity I, 150 mesh) was degassed under vacuum prior to use. The latter was mixed under nitrogen with the appropriate amount of water to reach the activity desired. All other reagents were obtained from the usual commercial suppliers and used as received. IR stretching frequencies were measured in solution or KBr discs. Nuclear Magnetic Resonance (NMR) spectra were routinely recorded at 300.13 (^{1}H), 121.50 (^{31}P{^{1}H}), or 75.47 MHz (^{13}C{^{1}H}) at 290 K in C_6D_6 solutions unless otherwise stated. Chemical shifts (δ) are given in ppm, relative to internal tetramethylsilane (^{1}H, ^{13}C) or external 85% aqueous H_3PO_4 (^{31}P). Coupling constants (J) are given in Hz.

Preparation of [MnRuCpCp′(μ-CO)$_2$(CO)(NO)] (6). Compound **1** (0.097 g, 0.315 mmol) was added to a tetrahydrofuran solution of compound **3**, freshly prepared from $[Ru_2Cp_2(CO)_4]$ (0.070 g, 0.157 mmol) and then cooled at 223 K, and the mixture was stirred for 1.5 h while allowing it to reach room temperature slowly. The solvent was then removed under vacuum, the residue was extracted with toluene, and the extracts were filtered through a 3 cm alumina pad (activity IV). After reducing the volume of the filtrate to about 3 mL, a layer of petroleum ether (15 mL) was added, and the mixture was stored at 253 K for 1 day to yield orange-brown crystals of compound **6** (0.068 g, 52%). Anal. Calcd for $C_{14}H_{12}MnNO_4Ru$: C, 40.49; H, 2.91; N, 3.37. Found: C, 40.40; H, 2.82; N, 2.94. ^{1}H NMR: δ 4.78 (s, 5H, Cp), 4.44 (m, 2H, C_5H_4), 4.20 (false t, $J_{HH}+J_{HH'}=4$, 2H, C_5H_4) 1.76 (s, 3H, Me). ^{13}C{^{1}H} NMR (100.63 MHz, CD_2Cl_2, 291 K): δ 245.8 (br, CO), 110.5 [s, $C^1(C_5H_4)$], 95.3, 95.2 [2 × s, $C^{2,3}(C_5H_4)$], 91.5 (s, Cp), 13.1 (s, Me). ^{13}C{^{1}H} NMR (100.63 MHz, CD_2Cl_2, 223 K): δ 271.2 (br, μ-CO, *trans* and *cis* isomers), 198.3, 197.5 (2 × s, RuCO, *trans* and *cis* isomers), 110.8 [br, $C^1(C_5H_4)$], 95.3 [br, $C^{2,3}(C_5H_4)$], 91.6 (s, br, Cp), 13.6 (s, Me). ^{13}C{^{1}H} NMR (100.63 MHz, CD_2Cl_2, 203 K): δ 271.7 (br, μ-CO, *trans* and *cis* isomers), 198.4, 197.6 (2 × s, RuCO, *trans* and *cis* isomers), 111.4, 110.8 [2 × s, $C^1(C_5H_4)$, *trans* and *cis* isomers], 95.8, 95.3 [2 × s, br $C^{2,3}(C_5H_4)$], 92.2, 91.5 (2 × s, Cp, *trans* and *cis* isomers), 13.7 (s, br, Me).

Preparation of [MoReCpCp′(μ-N)(CO)$_4$] (7a). A solid sample of compound **4a** was prepared in situ from $[Mo_2Cp_2(CO)_6]$ (0.040 g, 0.082 mmol). Compound **2** (0.072 g, 0.164 mmol) was then added, and the flask was cooled to 223 K. Precooled (at 223 K)

(32) Armarego, W. L. F.; Chai, C. *Purification of Laboratory Chemicals*, 5th ed.; Butterworth-Heinemann: Oxford, U.K., 2003.
(33) Connelly, N. G. *Inorg. Synth.* **1974**, *15*, 91.
(34) Tam, W.; Liu, G. Y.; Wang, K. W.; Kiel, W. A.; Wong, V. K.; Gladysz, J. A. *J. Am. Chem. Soc.* **1982**, *104*, 141.
(35) Dessy, R. E.; Weissman, P. M.; Pohl, R. L. *J. Am. Chem. Soc.* **1966**, *88*, 5117.
(36) Gladysz, J. A.; Williams, G. M.; Tam, W.; Johnson, D. L.; Parker, D. W.; Selover, J. C. *Inorg. Chem.* **1979**, *18*, 553.

Table 4. Crystal Data for Compound **9b**

mol formula	$C_{17}H_{21}NO_6PReW$
mol wt	736.37
cryst syst	triclinic
space group	$P\bar{1}$
radiation (λ, Å)	0.71073
a, Å	9.864(5)
b, Å	14.541(6)
c, Å	8.105(5)
α, deg	92.99(2)
β, deg	113.68(2)
γ, deg	97.68(2)
V, Å^3	1047.9(9)
Z	2
calcd density, g cm^{-1}	2.33
absorp coeff., mm^{-1}	11.362
temperature, K	293(2)
θ range, deg	3.08 to 29.99
index ranges (h, k, l)	−13, 12; −20, 18; 0, 11
no. of reflns collected	2428
no. of indep reflns (R_{int})	2428 (0.000)
no. of reflns with $I > 2\sigma(I)$	1773
R indexes[a] [data with $I > 2\sigma(I)$]	$R_1 = 0.0507$, $wR_2 = 0.1024$
R indexes[a] (all data)	$R_1 = 0.1647$, $wR_2 = 0.1578$
GOF	1.186
no. of restraints/ parameters	78/178
$\Delta\rho$(max,min), e Å^{-3}	2.309, −4.032

[a] $R_1 = \sum||F_o| - |F_c||/\sum|F_o|$, $wR_2 = [\sum[w(F_o^2 - F_c^2)^2]/\sum[w(F_o^2)^2]]^{1/2}$, $w = 1/[\sigma^2(F_o^2) + (aP)^2 + bP]$, where $P = [\max(F_o^2,0) + 2F_c^2]/3$.

dichloromethane (25 mL) was then added to that flask using a canula, and the dark red resulting suspension was stirred for 1.5 h while allowing it to reach room temperature slowly. The solvent was then removed under vacuum, the residue was extracted with toluene-petroleum ether (1:2), and the extracts were filtered through diatomaceous earth. Removal of the solvents under vacuum gave compound **7a** as a red-purple powder. Crystallization of this product from toluene-petroleum ether at 253 K yielded compound **7a** as red-black needles (0.071 g, 78%). Anal. Calcd for $C_{15}H_{12}MoNO_4Re$: C, 32.61; H, 2.19; N, 2.53. Found: C, 32.92; H, 2.21; N, 2.61. ^{1}H NMR: δ 4.98 (s, 5H, Cp), 4.64, 4.48 (2 × false t, $J_{HH} + J_{HH'} = 4$, 2 × 2H, C_5H_4), 1.67 (s, 3H, Me).

Preparation of [MoReCpCp′(μ-N)(CO)$_3${P(OMe)$_3$}] (7b). A solid sample of compound **4b** was prepared in situ from [$Mo_2Cp_2(CO)_4${P(OMe)$_3$}$_2$] (0.034 g, 0.050 mmol). Compound **2** (0.045 g, 0.100 mmol) was then added, and the flask was cooled to 213 K. Precooled (at 213 K) dichloromethane (25 mL) was then added to that flask using a canula, and the brown-orange resulting suspension was stirred for 2 h while allowing it to reach room temperature slowly. The solvent was then removed under vacuum, the residue was extracted with toluene-petroleum ether (1:1), and the extracts were filtered through a 3 cm alumina pad (activity IV). Removal of the solvents under vacuum gave compound **7b** as an orange powder. Crystallization of this product from toluene-petroleum ether at 253 K yielded compound **7b** as red-orange crystals (0.060 g, 79%). Anal. Calcd for $C_{17}H_{21}MoNO_6PRe$: C, 31.48; H, 3.26; N, 2.16. Found: C, 31.52; H, 3.19; N, 2.20. ^{1}H NMR: δ 5.14 (s, 5H, Cp), 4.72, 4.70 (2 × m, 2 × 1H, C_5H_4), 4.60 (m, 2H, C_5H_4), 3.61 (d, $J_{PH} = 12$, 9H, OMe), 1.67 (s, 3H, Me). ^{31}P{^{1}H} NMR: δ 189.7 (s).

Preparation of [MoReCpCp′(μ-N)(CO)$_3$(PPh$_3$)] (7c). The procedure is identical to that described for compound **7b**. By using compound **4c**, prepared from [$Mo_2Cp_2(CO)_4(PPh_3)_2$] (0.048 g, 0.050 mmol), and 0.045 g of compound **2** (0.100 mmol), red-orange crystals of compound **7c** were thus obtained (0.061 g, 75%). Anal. Calcd for $C_{32}H_{27}MoNO_3PRe$: C, 48.85; H, 3.46; N, 1.78. Found: C, 49.12; H, 3.46; N, 1.65. ^{1}H NMR: δ 7.8−7.1 (m, 15 H, Ph), 5.06 (s, 5H, Cp), 4.78, 4.52 (2 × m, 2 × 1H, C_5H_4), 4.68 (m, 2H, C_5H_4), 1.89 (s, 3H, Me). ^{31}P{^{1}H} NMR: δ 62.1 (s). ^{13}C{^{1}H} NMR (CD_2Cl_2): δ 254.2 (d, $J_{CP} = 12$, MoCO), 204.9, 204.1 (2 × s, ReCO), 136.2 [d, $J_{PC} = 44$, C^1(Ph)], 133.9 [d, $J_{PC} = 12$, C^2(Ph)], 130.5 [s, C^4(Ph)], 128.8 [d, $J_{PC} = 10$, C^3(Ph)], 108.2 [s, C^1(C_5H_4)], 96.0 (s, Cp) 85.7, 85.5, 85.3, 84.8 (4 × s, C_5H_4), 13.8 (s, Me).

Preparation of [WMnCpCp′(μ-N)(CO)$_4$] (8). The procedure is identical to that described for compound **7a**. By using compound **5a**, prepared from [$W_2Cp_2(CO)_6$] (0.050 g, 0.075 mmol), and 0.044 g of compound **1** (0.150 mmol), compound **8** was thus obtained as red-black needles (0.047 g, 61%). Anal. Calcd for $C_{15}H_{12}MnNO_4W$: C, 35.92; H, 2.37; N, 2.75. Found: C, 35.72; H, 2.41; N, 2.64. ^{1}H NMR: δ 4.91 (s, 5H, Cp), 4.17, 3.97 (2 × m, 2 × 2H, C_5H_4), 1.61 (s, 3H, Me).

Preparation of [WReCpCp′(μ-N)(CO)$_4$] (9a). The procedure is identical to that described for compound **7a**. By using compound **5a**, prepared from [$W_2Cp_2(CO)_6$] (0.050 g, 0.075 mmol), and 0.066 g of compound **2** (0.150 mmol), purple-black needles of compound **9a** were thus obtained (0.072 g, 74%). Anal. Calcd for $C_{15}H_{12}MnNO_4W$: C, 35.92; H, 2.37; N, 2.75. Found: C, 35.72; H, 2.41; N, 2.64. ^{1}H NMR: δ 4.91 (s, 5H, Cp), 4.66, 4.53 (2 × false t, $J_{HH} + J_{HH'} = 4$, 2 × 2H, C_5H_4), 1.67 (s, 3H, Me). ^{13}C{^{1}H} NMR (CD_2Cl_2, 100.63 MHz): δ 226.1 (s, $J_{CW} = 212$, WCO), 203.4 (s, ReCO), 110.0 [s, C^1(C_5H_4)], 95.0 (s, Cp), 91.7, 89.5 [2 × s, C^{2,3}(C_5H_4)], 14.0 (s, Me).

Preparation of [WReCpCp′(μ-N)(CO)$_3${P(OMe)$_3$}] (9b). The procedure is identical to that described for compound **7b**. By using compound **5b**, prepared from [$W_2Cp_2(CO)_4${P(OMe)$_3$}$_2$] (0.043 g, 0.050 mmol), and 0.045 g of compound **2** (0.100 mmol), red-orange crystals of compound **9b** were thus obtained (0.056 g, 76%). Anal. Calcd for $C_{17}H_{21}NO_6PReW$: C, 27.72; H, 2.87; N, 1.90. Found: C, 27.79; H, 2.91; N, 1.89. ^{1}H NMR: δ 5.06 (s, 5H, Cp), 4.73, 4.72 (2 × m, 2 × 1H, C_5H_4), 4.65 (m, 2H, C_5H_4), 3.62 (d, $J_{PH} = 12$, 9H, OMe), 1.80 (s, 3H, Me). ^{31}P{^{1}H} NMR: δ 161.5 (s).

Computational Details. Quantum chemical computations were carried out with the Gaussian 03 series of programs[37] using the hybrid density functional B3LYP,[38−40] which combines Becke's three-parameter nonlocal hybrid exchange potential with the nonlocal correlation functional of Lee, Yang, and Parr. A grid with 99 radial shells around each atom and 302 angular points per shell was used in the numerical calculations of the exchange-correlation potential. Stable species and transition states (TS) were fully optimized in the gas phase by using the LANL2DZ basis set for Mn, Ru, and W atoms,[41] and the 6−31G(d) basis set[42] for the remaining atoms, and the standard Schlegel algorithm.[43] The nature of the stationary points was verified by analytical computations of harmonic vibrational frequencies. IRC calculations starting at each saddle point verified the two minima connected by that TS by using the Gonzalez and Schlegel method implemented in Gaussian 03.[44,45] A statistical thermodynamics treatment was also carried out to calculate ΔH, ΔS, and ΔG at a pressure of 1 atm and a temperature of 253.15 K within the ideal gas, rigid rotor and harmonic oscillator approximations.[46]

To take into account condensed-phase effects we used the Polarizable Continuum Model (PCM)[47−50] of Tomasi et al. with the united atom Hartree−Fock (UAHF) parametrization.[49] The solvation Gibbs energies ΔG_{solv} along the reaction coordinate were evaluated from single-point PCM-UAHF calculations on the gas phase geometries. Addition of the relative solvation Gibbs energy

(37) Frisch, M. J. et al. *Gaussian 03*, Revision B.04; Gaussian, Inc.: Pittsburgh, PA, 2003.
(38) Becke, A. D. *Phys. Rev. A* **1988**, *38*, 3098.
(39) Lee, C.; Yang, W.; Parr, R. G. *Phys. Rev. B* **1988**, *37*, 785.
(40) Becke, A. D. *J. Chem. Phys.* **1993**, *98*, 5648.
(41) Hay, P. J.; Wadt, W. R. *J. Chem. Phys.* **1985**, *82*, 299.

$\Delta\Delta G_{solv}$ to ΔG_{gas} gives ΔG_{sol} (see Supporting Information). A relative permittivity of 7.58 was assumed in the calculations to simulate tetrahydrofuran as the solvent used in the experimental work.

The Kohn−Sham determinants of the most important critical structures located along the reaction coordinate were also studied by means of a theoretical method developed by the Fukui's group.[51] This method is based on the expansion of the MOs of a complex system, AB, in terms of the MOs of its constituent fragments, A and B, using the geometry of each fragment in the corresponding critical structure and the performance of the configurational analysis. The configurational analysis is performed by writing the determinant constructed by the Kohn−Sham MOs of the complex system, Ψ, by a combination of various fragment electronic configurations:

$$\Psi = C_0\Psi_0 + \sum C_q\Psi_q$$

where Ψ_0 (zero configuration, AB) is the state in which neither electron transfer nor electron excitation takes place and Ψ_q stands for monotransferred configurations, $\Psi_{o\rightarrow u'}$, in which one electron in an occupied MO, o, in one of the two fragments A or B is transferred to an unoccupied MO, u′, of the other fragment (A^+B^-, and A^-B^+ configurations), monoexcited configurations, $\Psi_{o\rightarrow u}$, in which one electron in an occupied MO, o, of any of the two fragments is excited to an unoccupied MO, u, of the same fragment (A*B and AB* configurations), and so on. This configuration analysis which has proved useful for understanding the physicochemical features of chemical interactions was performed by means of the ANACAL program.[52]

X-ray Structure Determination for Compound 9b. Full crystallographic data for **9b** are provided in the CIF file format, while Table 4 summarizes the most relevant crystal data for this structural study. Data collection was performed with a Philips PW 1100 diffractometer (Mo Kα; $\lambda = 0.71073$ Å), and cell constants were obtained from a least-squares refinement of the setting angles of 24 randomly distributed and carefully centered reflections ($8.49 < 2\theta < 17.68$). No crystal decay was observed and an absorption correction using the method of Walker and Stuart was applied,[53] which gave minimum and maximum transmission factors of 0.650 and 1.000. The structure was solved by direct methods (SIR97),[54] and refined with full-matrix least-squares (SHELXL-97),[55] using the WinGX software package.[56] Because of the poor quality of the crystal, only W, Re, N, P, and the C atoms of the Cp rings were refined anisotropically, whereas the remaining atoms were refined isotropically. Each of the $O-CH_3$ groups of the trimethyl phosphite was found disordered and distributed in two positions with site occupancy factors of 0.3 and 0.7, respectively, after refinement. Graphical material was prepared with the ORTEP3 for Windows program.[57]

Acknowledgment. We thank the MEC of Spain and Principado de Asturias, Spain, for financial support (Projects CTQ2006-01207 and PA-MAS94-05).

Supporting Information Available: Full crystallographic data for **9b** in CIF file format. Complete reference 37. Figures showing the optimized geometries and selected bond lengths and angles for all species involved in the reactions of the cation $[MnCp(CO)_2(NO)]^+$ with the anions $[WCp(CO)_3]^-$ and $[RuCp(CO)_2]^-$, and a listing of the corresponding Cartesian coordinates, as well as tables of the corresponding Gibbs energies and (in the case of all located transition states) imaginary vibrational frequencies (PDF). This material is available free of charge via the Internet at http://pubs.acs.org.

IC801356M

(42) Hehre, W. J.; Radom, L.; Pople, J. A.; Schleyer, P. v. R. *Ab Initio Molecular Orbital Theory*; Wiley: New York, 1986.
(43) Schlegel, H. B. *J. Comput. Chem.* **1982**, *3*, 214.
(44) Gonzalez, C.; Schlegel, H. B. *J. Chem. Phys.* **1989**, *90*, 2154.
(45) Gonzalez, C.; Schlegel, H. B. *J. Phys. Chem.* **1990**, *94*, 5523.
(46) McQuarrie, D. A. *Statistical Mechanics*; Harper & Row: New York, 1986.
(47) Tomasi, J.; Persico, M. *Chem. Rev.* **1994**, *94*, 2027.
(48) Cossi, M.; Barone, V.; Cammi, R.; Tomasi, J. *Chem. Phys. Lett.* **1996**, *255*, 327.
(49) Barone, V.; Cossi, M.; Tomasi, J. *J. Chem. Phys.* **1997**, *107*, 3210.
(50) Tomasi, J.; Cammi, R. *J. Comput. Chem.* **1998**, *19*, 404.
(51) Fujimoto, H.; Kato, S.; Yamabe, S.; Fukui, K. *J. Chem. Phys.* **1974**, *60*, 572.
(52) López, R.; Menéndez, M. I.; Suárez, D.; Sordo, T. L.; Sordo, J. A. *Comput. Phys. Commun.* **1993**, *76*, 235.
(53) Walker, N.; Stuart, D. *Acta Crystallogr.* **1983**, *A39*, 158.
(54) Altomare, A.; Burla, M. C.; Camalli, M.; Cascarano, G. L.; Giacovazzo, C.; Guagliardi, A.; Moliterni, A. G. G.; Polidori, G.; Spagna, R. *J. Appl. Crystallogr.* **1999**, *32*, 115.
(55) Sheldrick, G. M. *SHELXL97: Program for the Refinement of Crystal Structures*, Release 97−2; University of Göttingen: Göttingen, Germany, 1997.
(56) Farrugia, L. J. *J. Appl. Crystallogr.* **1999**, *32*, 837.
(57) Farrugia, L. J. *J. Appl. Crystallogr.* **1997**, *30*, 535.